Changes of protein stiffness during folding detect protein folding intermediates

Katarzyna E. Małek · Robert Szoszkiewicz

How to cite this manuscript

Published Version Information

Changes of protein stiffness during folding detect protein folding intermediates

Katarzyna Małek, Robert Szoszkiewicz

Department of Physics, Kansas State University, Manhattan, KS 66506-2601, USA

E-mail: `rs@phys.ksu.edu`

Abstract. Single molecule force-quench atomic force microscopy (FQ-AFM) is used to detect folding intermediates of a simple protein by detecting changes of molecular stiffness of the protein during its folding process. Those stiffness changes are obtained from shape and peaks of an autocorrelation of fluctuations in end-to-end length of the folding molecule. The results are supported by predictions of the equipartition theorem and agree with existing Langevin dynamics simulations of a simplified model of a protein folding. In the light of the Langevin simulations the experimental data probe an ensemble of random-coiled collapsed states of the protein, which are present both in the force-quench and thermal-quench folding pathways.

Introduction

Protein folding relates to many diseases such as Creutzfeld-Jacob disease, Alzheimers disease, Huntington's disease and Parkinson's disease [1, 2]. Despite knowing the major forces involved in the folding process its details were considered one of the big questions over the next quarter-century by 2005 *Science Magazine.* There is an astronomically large number of folding pathways available for even small proteins and the folding environment *in vivo* is crowded by many other molecules, which can either help, hinder, or divert this process [3, 4, 5].

Single molecule experiments, and AFM studies in particular, are potentially well suited to address protein folding at the single molecule level [6, 7, 8]. However, temporal resolution of these experiments is still insufficient to resolve folding intermediates, particularly in the case of simple proteins. But structural changes along the folding process for simple proteins with only few units of secondary structure are expected to bring critical advancements in understanding protein folding [9]. For example, Garcia-Manyes et al. [10] were able to detect an ensemble of the collapsed, but not-yet-folded states in two monomeric and multi-domain proteins by manipulating protein molecules using mechanical force. By varying the time a refolding molecule spends in the quenched force regime, an ensemble of resolvable steps in the end-to-end length of a protein was detected when the protein did not have enough time to collapse and fold completely.

In this manuscript we report how to measure changes in mechanical stiffness of *in situ* folding protein, and show that those changes can serve to detect protein folding intermediates. Transient stiffnesses are detected from shape and peaks in the autocorrelation function calculated from fluctuations in the end-to-end length of a folding molecule. These results are supported by the equipartition theorem, and agree with predictions of recent Langevin dynamics simulations, which suggested an ensemble of the collapsed random-coiled states as necessary intermediate states in force controlled protein folding.

Materials and Methods

A simple recombinant protein with four identical I27 molecules connected by arginine-serine linkers in tandem is used here. I27 is the 27th domain of a human cardiac titin and has only 89 residues. Its secondary structure is 33 % beta–type and otherwise unstructured [11, 9]. I27 folds into an immunoglubilin-like fold, which is one of the most common structural motifs in the pdb protein database. Consequently, I27 (un)folding has been thoroughly studied *in ensemble* and by single molecule techniques [7, 9, 8, 10].

The gene of $I27_4$ was obtained from several rounds of in-cloning of I27 DNA into pQE30 plasmid from Qiagen [12]. $I27_4$ protein was expressed in *E.coli* XL1-Blue cells, purified in Talon-Co^{2+} gravity column, dialysed into Dulbecco phosphate-buffered saline buffer (DPBS), and stored at 4 ^{o}C at a concentration of 1 mg/ml [12]. Good quality of $I27_4$ purification was verified by SDS-PAGE. Protein samples deposited on gold

evaporated glass slides were used for the FQ-AFM studies with MLCT-C cantilevers from Bruker. Extensive details about this FQ-AFM setup are presented in the Ref. [12].

Results and Discussion

Each structure, and hence each single molecule as well, has its own proper set of mechanical properties. One of such properties is the elastic stiffness, k, which relates changes of extension/contraction x of a molecule due to a small pulling/compressive force vector $\vec{F}$. The value of k along a pulling/compressive direction is thus $k = \partial F/\partial x$.

In this work we propose a novel way of finding protein folding intermediates by exploring changes in the elastic stiffness k of protein molecules, which are initially stretched and unfolded by a mechanical force at the single molecule level, and then try to refold once a stretching force is slowly relaxed. To illustrate our approach we use a simple protein, which is well biochemically characterized and folds into only one type of a secondary structure. To unfold and provide a chance for slow refolding of our protein of interest we employ the FQ-AFM method. Folding times of simple proteins such as ubiquitin, ankyrin, spectrin, and I27 were extended 10,000 times from ms in ensemble to tens of seconds in FQ-AFM setups [8]. By analogy, we expect to detect in our FQ-AFM experiments an ensemble of folding intermediates with lifetimes much longer than sub-ms, which in solution/bulk folding experiments are unnoticed.

Fig. 1 explains how a single $I27_4$ molecule is manipulated using FQ-AFM. Temporal changes in the end-to-end length of a protein, L, are measured while monitoring the changes of a tensile clamping force, F. Initial unfolding events of each domain of I27 within the $I27_4$ molecule are observed in a stepwise increase of L with time. Upon a slow force quench, the molecule tries to refold, and it often fails to do so as verified in its continuous non step-like length increase upon a force increase. See Suppl. Data for an extensive gallery of FQ-AFM traces.

By analyzing a zone marked as the *region of interest* in Fig. 1(B) mean square fluctuations of end-to-end length of a re-folding $I27_4$ are obtained. First, instantaneous changes of L with time, $\Delta L(t)$, are calculated from polynomial fits to smoothed L vs. time data using time steps of 1 ms.‡ A chosen time step is an inverse of the 1 kHz bandwidth (BW). The values of ΔL are divided by corresponding values of ΔF obtained from smoothed and line-fitted F vs. time traces to yield values of instantaneous compliance of a folding protein. Mean square fluctuations of L about its mean, $< \Delta x^2 >$, are calculated by squaring the actual fluctuations of L about its polynomial-fitted and smoothed mean in 1 ms time windows. The result of averaging $< \Delta x^2 >$ vs. $\Delta L/\Delta F$ for 66 non-refolders is plotted in Fig. 2(A).

Before analyzing the data in Fig. 2, expected stiffnesses of unfolded and folded I27

---

‡ Typically a polynomial between 7th order (8 terms) and 12th order (13 terms), was fitted to smoothed L vs. time curves. This was done to subtract a fitted L from an actual and fluctuating L. The procedure was to start with the smallest order of a polynomial, and increase it until a fit goodness (measured with a χ^2) would not change by more than several per cent.
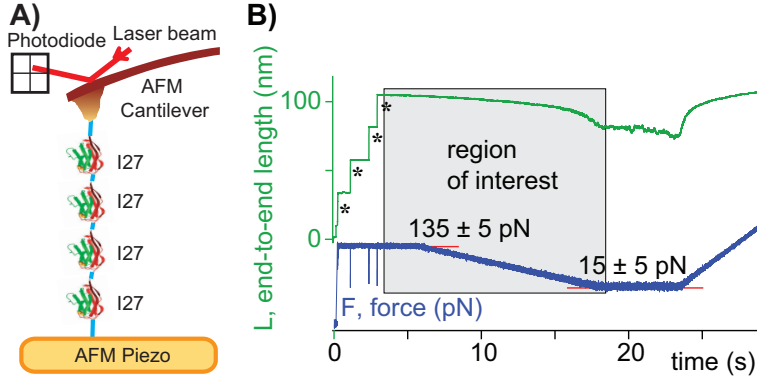
Figure 1. I27$_4$ refolding in the force-quench (FQ-AFM) mode. A) Schematic illustration of single I27$_4$ clamped between an AFM tip and a gold substrate. B) FQ-AFM traces corrected for AFM cantilever bending. After complete unfolding of I27$_4$ at 135 ± 5 pN tensile force (marked by 24 nm steps in the proteins end-to-end length L) the protein is left to refold by slowly quenching the force to 15 ± 5 pN. An example of a non-refolder is presented. Non-refolders lack re-unfolding steps in L vs. time trace when the force is ramped up back to 135 pN after about 23 s.
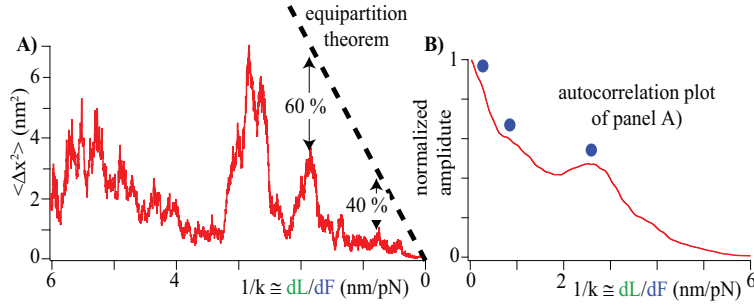

Figure 2. Analysis of the non-refolding I27$_4$. A) Mean square fluctuations of L about its mean, $< \Delta x^2 >$, for 66 non-refolders is plotted as a function of ΔL over ΔF at each point of the non-refolding trajectory in the region of interest marked in Fig. 1. The value of ΔL over ΔF corresponds to the cantilever-protein compliance, or an inverse of a corresponding normal spring constant. A dashed line plots the predictions of Eq. 3. As the compliances grow more fluctuations are recovered, i.e., from about 40 % of $k_B T$ at compliances of about 0.7 nm/pN to about 60 % of $k_B T$ at compliances of about 2 nm/pN. B) The autocorrelation function of the panel (A) shows several predominant maxima, which are marked by blue circles.

are reviewed. Using the worm-like chain (WLC) model of polymer elasticity compliance of a stretched and unfolded I27$_4$ molecule is estimated. The WLC model, which is used widely to infer protein elasticity [6, 7, 12], relates the protein extension x with force F acting on a protein:

$$F = k_B T \left[0.25(1 - x/L_o)^{-2} - 0.25 + x/L_o \right] /p. \tag{1}$$

The elastic stiffness k of a protein is:

$$k = \partial F/\partial x = k_B T \left[(1 - x/L_o)^{-3} + 2 \right] /(2 * p * L_o), \tag{2}$$

Here, k_B is the Boltzmann's constant and T is the absolute temperature. Thus, from

Eqs. 1 & 2 the elastic spring constant of 15 pN/nm is obtained for an *unfolded* $I27_4$ protein stretched by 135 pN tensile force and when using a typical persistence length p of 0.36 nm and $I27_4$ contour length L_o of 128 nm [6, 7, 12].

However, an issue of an elastic spring constant k_f of a *folded* I27 and other proteins is unsettled and still in its infancy. There is a very limited number of experimental measurements and contradictory results depend on the observation method and the type of an analysis. Several recent reports yield the values of k_f between several pN/nm to a few tens of pN/nm [6, 13, 14, 18]. However, since an elastic stiffness of a covalent bond is about 10,000 pN/nm, the values of elastic spring constants of folded proteins reported by Dietz et al. [15], which are of about 1,000 pN/nm, are also entirely plausible. We argue in the Supplementary Materials that those high values of elastic spring constants are obtained in the limit of a stretched and just-about-to-unfold protein and using several approximations. Thus, we would rather associate those values with elastic spring constants of a harmonic unfolding potential for a stretched protein.

Overall, during folding of $I27_4$ from its extended state, a monotonic decrease of the spring constant from about 15 pN/nm to several pN/nm is expected due to a force decrease. At the same time any transient folding event is expected to produce transient structures, i.e., local peaks in the stiffness vs. time curve, with stiffnesses between several to a few tens of pN/nm. Thus, both the shape of stiffness vs. time dependence as well as any transient compliances of less than 1 nm/pN are of particular interest, since they can pinpoint transient folding structures.

Fig. 2(B) plots an autocorrelation of a plot in Fig. 2(A) using our resolution time step of 1 ms. This yields most pronounced values of molecular compliances found during a $I27_4$ re-folding process. The autocorrelation plot in Fig. 2(B) is rather smooth and shows three most pronounced molecular compliances of about 0.4 nm/pN, 1 nm/pN and 3 nm/pN. However, based on the aforementioned predictions, one would like to concentrate on compliances of less than 1 nm/pN, i.e., stiffnesses of more than 1 pN/nm. These are plotted in Figure 3 after analyzing selectively FQ-AFM traces with only one, two, three, and four unfolded I27 domains.

When the protein is stretched almost to its contour length, i.e., when the term $(1 - x/L_o)^{-3}$ from Eq. 2 is dominant, the ratio of F over k depends linearly on x. Thus, for an observed parabolic decrease of x with time in Fig. 1(B) one expects a monotonous hyperbolic-like decrease of entropic elasticity for a collapsing protein. However, beyond such monotonous decrease several transient values of k are clearly observed in Fig. 3. These can indicate intermediate states during a protein folding process, which due to an experimental bandwidth of 1 ms must have lasted for at least several ms. Since folding of each I27 molecule is a guided, but yet stochastic process [16], these peaks are best visible when only very few folding trajectories are averaged. This is why sharp peaks are only observed when just a few, e.g., up to about 10 traces are averaged, which is the case of one and four domains of $I27_4$ being folded respectively. Smoothed and not very well distinguishable peaks are observed when 25 traces are averaged, which is the case of two and three domains of $I27_4$ being folded respectively.
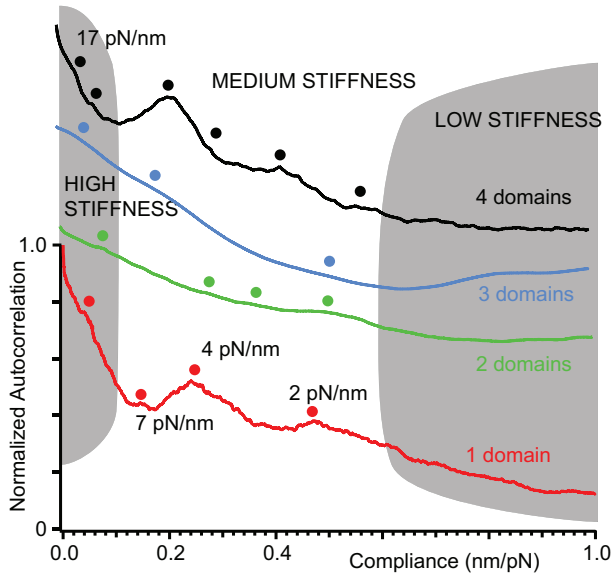
Figure 3. The autocorrelation plots like in Fig. 2(B), but obtained after averaging N FQ-AFM results of $< \Delta x^2 >$ vs. $\Delta L/\Delta F$ with respectively one ($N = 10$), two ($N = 25$), three ($N = 25$), and four ($N = 6$) I27$_4$ domains captured and extended by an AFM tip. Each single FQ-AFM L vs. time trace has a different upper limit of the molecular compliance. Thus, each autocorrelation was carried up to a point where at least three traces contributed. The autocorrelation plots for more than one domains are vertically shifted. Arbitrary defined zones of high and low stiffnesses with $k > 10$ pN/nm and $k < 2$ pN/nm are shaded. First derivative of the autocorrelation functions were used to identify the respective maxima marked by filled circles. Multiplicities of the same compliances were excluded from this analysis. Noteworthy, the I27 modules did not aggregate while being manipulated by FQ-AFM. This was verified by the re-unfolding phase in the FQ-AFM traces, and likely helped by the slow force quench process, similarly as in Ref. [7].

We have also analyzed 13 refolding traces: two traces with one domain refolding, four traces with two domains refolding, four traces with three domains refolding, and three traces with four domains refolding. Our analysis of those refolders extended down to their highly collapsed lengths, but did not probe a constant force-quenched zone of 15 ± 5 pN, see Fig. 1(B), due to artifacts, which would arise from $\Delta F \simeq 0$ in that zone. Supplementary figures S9-S12 depict several examples of refolders. Supplementary figures S13-S16 show the results of our analysis for those refolders. The results obtained for the refolders are similar to the results obtained for the non-refolders in the Fig. 3. This is consistent with the fact that we are unable to probe an ensemble of folded and almost-folded I27 structures, and thus the results for highly collapsed non-refolders are expected to match the results for refolders.

Overall, both for non-refolders and refolders only a few distinct stiffnesses are detected. This set includes several molecular stiffnesses around 20 pN/nm, several stiffnesses between 7 pN/nm and 2 pN/nm, and possibly a few stiffnesses around 1 pN/nm, but provided that these are not multiplications of any earlier peaks.

Despite several approaches in the literature [17, 13, 14, 18], an adequate model to

confirm findings in Fig. 3 by extracting viscoelasticity of the protein being pulled by the AFM cantilever in the FQ-AFM mode is missing. While stiffness of the AFM cantilever remains unchanged, such a model must take into account that the elastic stiffness and viscous damping of the protein depend on its extension and its state, i.e., folded vs. unfolded. However, dwelling on the existing approaches, mechanical coupling between a protein molecule and an AFM cantilever is expected to produce two major effects. First, frequency spectrum of mechanical vibrations of the $I27_4$ molecule will depend on the stresses and extensions induced by an AFM cantilever. Second, a frequency spectrum of mechanical vibrations of the AFM cantilever will change accordingly.

To find out any vibrational modes of whole $I27_4$ molecules fourier transforms of the molecular length and clamping forces, i.e., L vs. time and F vs. time, respectively, were evaluated using 1 kHz experimental BW. No novel resonance modes beyond the electrical instrumental noise of 60 Hz and its multiplicities were observed, see the Suppl. Data. Those observations are explained as follows. Molecular elasticity of a protein is associated with its normal vibrational modes at frequencies f_i^p, which relate to protein elasticity k_i^p and its effective mass m_i^p at a given i-th mode, so that: $2\pi f_i^p = (k_i^p/m_i^p)^{1/2}$. The largest measured values of transient stiffnesses in Fig. 3 similar as elastic spring constants of cantilever used here, i.e., 15 pN/nm §, but an effective mass of a protein is much smaller than that of an AFM cantilever. A resonance frequency of a first MLCT-C cantilever mode in water is between one to several kHz. Thus, it is expected that a resonance frequency of a first vibrational mode of the protein is much larger than that [12]. Khatri et al. [13] found out that the relaxation time constants necessary for unfolded I27 molecules to relax upon a force change in a range of tensile forces between 15 to 200 pN are about 0.03 ± 0.03 ms. The relaxation time constants relate to the damping coefficient (expressed in 1/s) of the first resonance mode for unfolded I27 [19]. This implies that a first mechanical resonance of the mechanically stretched I27 occurs above 10 kHz. Same is expected for the first mechanical resonance of the folded I27 due to comparable elastic spring constants between folded and unfolded I27s. Furthermore, a normal mode analysis predicts first normal modes of small proteins to be in the MHz range [20]. Subharmonics of these normal modes within 1 kHz BW are not expected either. This is because transient not-yet-folded I27 structures must be short lived, i.e., have not been readily observed in experiments, so that their amplitudes in the frequency domains will be small.

Despite being undetectable below 1 kHz, any stiffness changes along an I27 folding trajectory shift resonances of an AFM cantilever [17, 13, 14, 18]. These shifts are observed in Fig. 2(A) when applying an equipartition theorem. From the equipartition theorem, thermal energy per one degree of freedom, $k_B T/2$, must be balanced by a mechanical energy dissipated in each i–th resonance mode of an AFM cantilever coupled to a protein. Such a mechanical energy relates to mean fluctuations in position of the AFM cantilever squared and integrated over a given mode. However, in the FQ-AFM

§ To be precise stiffnesses associated with 1st resonance modes of the AFM cantilevers should be referred to. These are at about 10 pN/nm.

mode, mean fluctuations in position of the AFM cantilever are exactly the same as fluctuations in an extended end-to-end length of a protein. Then, an equipartition theorem applied to the fluctuations squared of a mean protein end-to-end length, $< \Delta x^2 >$, yields:

$$(k_i < \Delta x^2 >)/2 = (k_B T)/2 \Longrightarrow < \Delta x^2 > = (k_B T)/k_i \qquad (3)$$

where: $k_i = \Delta F / \Delta L$ is a spring constant of the i–th resonance mode of a protein molecule coupled to an AFM cantilever and calculated along a one dimensional pulling coordinate.

A dashed line in Fig. 2(A) relates the values of $< \Delta x^2 >$ to the values of k_i as predicted by Eq. 3. As the compliance of an AFM cantilever coupled to the protein grows, more fluctuations are recovered, i.e., from about 40 % of $k_B T$ at compliances of about 0.7 nm/pN to about 60 % of $k_B T$ at compliances of about 2 nm/pN. These results agree with what has been observed for an unfolded I27 clamped under a range of forces from 100 pN to 300 pN [13]. Namely, increasing protein stiffness (smaller compliance) increases the resonance frequencies of an AFM cantilever coupled to the protein. This results in a decrease of vibrational amplitudes detected at quasi-static frequencies. In particular, a typical frequency of a first resonance of the MLCT-C cantilevers in water is about 1 kHz. After interactions with proteins, this frequency shifts much above 1 kHz, and thus only a fraction of $< \Delta x^2 >$ is detected within 1 kHz BW. The higher is the stiffness of a protein, the bigger is a frequency increase, and the smaller is a recorder fraction of $< \Delta x^2 >$. Overall, the intermediate stiffnesses are detected not only from the shape and peaks of the autocorrelation of the fluctuations in end-to-end lengths of the folding molecule; the equipartition theory suggest their presence as well.

Theoretical modeling in the works of Li et al. [21] and Camacho et al. [22] describes various types of the I27 folding intermediates, and among them the structures being far from native-like states. Experimentally, Garcia-Manyes et al. [10] found out that quenching and then increasing again the clamping force in the case of ubiquitin resulted in a detectable ensemble of not-yet-folded states. They found such states when the force quench phase lasted as little as several hundreds of ms. Those states were also found as necessary precursors for the fully folded states. Garcia-Manyes et al. extended those results to the I27 molecules. Therefore, those theoretical and experimental findings provided for us reasonable grounds to expect finding mechanical folding intermediates within not-yet-native-like structures.

As mentioned above, an ensemble of transient structures present during force-quenched I27 refolding was predicted based on the coarse-grained folding simulations of I27 molecule by Li et al. [21]. While upon temperature initiated folding the collapse and folding of I27 are synchronous, Li et al. suggested that refolding from stretched initial structures not only increases the folding and collapse time scales, but also decouples these processes. Initial mechanically stretched state in the force-quench refolding has a low conformational entropy, and upon a force quench it contracts to the ensemble of partially random-coiled states RC_f. For a slow force quench process, as in our

experiments, the RC_f ensemble of states has enough time to equilibrate with the states associated with the random-coiled states RC, which are present in the thermal quench pathway as well.

Thus, our measurements on highly collapsed non-refolders, as well as refolders, suggest that using the proposed here experimental method, we are able to probe the RC ensemble, and maybe the RC_f ensemble. As such our results confirm existence of the ensemble of mechanically collapsed states, which was probed differently by Garcia-Manyes et al. [10] and postulated by Camacho et al. [22]. The RC ensemble of states are thought to be a small subset with only few tens configurations [22]. Nevertheless, more structural information beyond measured here normal elasticities of a folding protein is needed to structurally characterize a given folding intermediate. Obtaining such an information, however, appears to be entirely possible. In addition to a measured here normal elasticity changes, a more complete picture would result from measuring molecular elasticities in other than normal directions. Then, additional modeling, like elastic network models [20, 23], can be used to relate elastic properties of the RC ensemble to the results of such studies.

Conclusions

In conclusion, intermediate stiffnesses are detected from shape and peaks in autocorrelation of the fluctuations in the end-to-end lengths of folding molecules, as well as by applying the equipartition theorem. These intermediates are likely probing the ensemble of collapsed random-coiled states also present in the thermal folding pathways. Studies with force clamp spectrometers using different pulling directions are expected to detail on nano-mechanical characterization of folding intermediates in the case of small proteins. Thus, together with elastic network models the structural details of the transient mechanical structures during folding of simple proteins are expected to be resolved.

Acknowledgments

References

[1] F. Chiti and C. M. Dobson. Protein misfolding, functional amyloid, and human disease. *Annual Review of Biochemistry*, 75:333–66, 2006.

[2] D. Thirumalai, D. K. Klimov, and R. I. Dima. Emerging ideas on the molecular basis of protein and. *Current Opinion in Structural Biology*, 13:146–59, 2003.

[3] E. Shakhnovich. Protein folding thermodynamics and dynamics: Where physics, chemistry, and. *Chemical Reviews*, 106:1559–88, 2006.

[4] Y. W. Chen, F. Ding, H. F. Nie, A. W. Serohijos, S. Sharma, K. C. Wilcox, S. Y. Yin, and N. V. Dokholyan. Protein folding: Then and now. *Archives of Biochemistry and Biophysics*, 469:4–19, 2008.

[5] J. Frydman. Folding of newly translated proteins in vivo: The role of molecular chaperones. *Annual Review of Biochemistry*, 70:603–47, 2001.

[6] M. Rief, M. Gautel, F. Oesterhelt, J. M. Fernandez, and H. E. Gaub. Reversible unfolding of individual titin immunoglobulin domains by AFM. *Science*, 267:1109–12, 1997.

[7] J. M. Fernandez and H. B. Li. Force-clamp spectroscopy monitors the folding trajectory of a single protein. *Science*, 303:1674–78, 2004.

[8] A. Borgia, P. M. Williams, and J. Clarke. Single-molecule studies of protein folding. *Annual Review of Biochemistry*, 77:101–25, 2008.

[9] J.-H. Han, S. Batey, A. A. Nickson, S. A. Teichmann, and J. Clarke. The folding and evolution of multidomain proteins. *Nature Reviews Molecular Cell Biology*, 8:321–30, 2007.

[10] S. Garcia-Manyes, L. Dougan, C. L. Badilla, J. Brujic, and J. M. Fernandez. Direct observation of an ensemble of stable collapsed states in the mechanical folding of ubiquitin. *Proceedings of the National Academy of Sciences of the United States of America*, 106:10534–9, 2009.

[11] S. Improta, A. S. Politou, and A. Pastore. Immunoglobulin-like modules from titin i-band: Extensible components of muscle elasticity. *Structure*, 4:323–37, 1996.

[12] A. Dey and R. Szoszkiewicz. Complete noise analysis of a simple force spectroscopy afm setup and its applications to study nanomechanics of mammalian notch 1 protein. *Nanotechnology*, 23:175101–15, 2012.

[13] B. S. Khatri, K. Byrne, M. Kawakami, D. J. Brockwell, D. A. Smith, S. E. Radford, and T. C. B. McLeish. Internal friction of single polypeptide chains at high stretch. *Faraday Discussions*, 139:35–51, 2008.

[14] Y. Taniguchi, B. S. Khatri, D. J. Brockwell, E. Paci, and M. Kawakami. Dynamics of the coiled-coil unfolding transition of myosin rod probed by. *Biophysical Journal*, 99:257–62, 2010.

[15] H. Dietz, F. Berkemeier, M. Bertz, and M. Rief. Anisotropic deformation response of single protein molecules. *Proceedings of the National Academy of Sciences of the United States of America*, 103:12724–8, 2006.

[16] J. D. Bryngelson and P. G. Wolynes. Intermediates and barrier crossing in a random energy model (with applications to protein folding). *J. Phys. Chem.*, 93:6902–15, 1989.

[17] C. A. Bippes, A. D. L. Humphris, M. Stark, D. J. Muller, and H. Janovjak. Direct measurement of single-molecule visco-elasticity in atomic force microscope force-extension experiments. *European Biophysical Journal*, 35:287–92, 2006.

[18] Y. Wang and G. Zocchi. The folded protein as a viscoelastic solid. *EPL*, 96:18003, 2011.

[19] R. Szoszkiewicz. Comment about "print your afm" paper. *Review of Scientific Instruments*, 83:037101, 2012.

[20] K. Eom. *Simulations in nanobiotechnology.* CRC Press, 2012.

[21] M. S. Li, C. K. Hu, D. K. Klimov, and D. Thirumalai. Multiple stepwise refolding of immunoglobulin domain i27 upon force quench depends on initial conditions. *Proceedings of the National Academy of Sciences of the United States of America*, 103:93–8, 2006.

[22] C. J. Camacho and D. Thirumalai. Minimum energy compact structures of random sequences of heteropolymers. *Physical Review Letters*, 71:2505–8, 1993.

[23] N. E. Hudson, F. Ding, I. Bucay, E. T OBrien III, O. V. Gorkun, R. Superfine, S. T. Lord, N. V. Dokholyan, and M. R. Falvo. Sub-microsecond elastic recoil reveals molecular origins of fibrin fiber mechanics. *Biophysical Journal*, 104:2671-2680, 2013.